Chapter 23

Numerical Simulation of Slab Broadening in Continuous Casting of Steel

Jian-Xun Fu and Weng-Sing Hwang

Additional information is available at the end of the chapter

http://dx.doi.org/10.5772/47768

1. Introduction

Broadening is the deformation of materials in the vertical direction of force in the steel rolling process. Slab broadening in continuous casting increases the slab width in the secondary cooling zone. Continuous casting is a process in which the temperature drops sharply. The drop in temperature leads to slab shrinkage; the linear shrinkage of carbon steel is about 2.5% in the width direction. The decrease in slab width from the initial shell to the cooling slab is considered to be almost negligible and the width may even increase under some conditions.

Although the slab shrinks in the secondary cooling zone, the width of the slab is sometimes greater than that of the entrance of the corresponding mold. The change in slab width is due to broadening being greater than shrinkage. It is rarely well-know that this phenomenon often occurs for slab in continuous casting. Slab broadening makes it difficult to accurately control the size of the slab and has adverse effects on the subsequent rolling processes. Slab broadening becomes increasingly obvious with increasing casting speed. If no vertical miller is used in the rolling process, the broad part of the slab is cut off, wasting material. With a vertical miller, the broad part of the slab is rolled in the width direction, which leads to fluctuation in the slab thickness. The study of slab broadening in the continuous casting process is thus necessary. The present work (FU JianXun et al. 2010(a-c),2011(a-b)) investigates slab broadening in continuous casting using mathematical simulation, industrial measurements, and experiments. Assessments of slab width in several continuous casting factories indicate that slab broadening is common in the continuous casting process. Slab broadening occurs in the secondary cooling zone, as confirmed by experiments. The effects of the productive factors on the slab broadening were also derived. The mechanism of slab broadening is investigated and discussed.

2. Research method

2.1. Index definition

In order to measure slab broadening, the ratio of apparent shrinkage (RAS) and the ratio of ultimate broadening (RUB) were defined respectively as:

$$RAS = \left(U / W - 1\right) \times 100\%, \tag{1}$$

$$RUB = \left(S / T - 1\right) \times 100\%, \tag{2}$$

where:
U is size of mold on the top entrance (mm);
W is the measured width of the slab (mm);
T is the ultimate width of the slab (in mm);
S is the width of the slab (in mm).

The value of the RAS, which denotes the degree of mold shrinkage, is positive when the top width exceeds the slab width. This index can be used to set the mold size. The value of the RUB, which denotes the degree of broadening, is positive when the slab width exceeds the ultimate width.

2.2. Online measurements

An online measurement system was designed to measure slab broadening at the exit of the caster.(FU JianXun et al. 2011(b)) The system comprises an optical lens, a digital camera, a data cable (IEEE 1394), and a computer. The system is controlled using the computer. The digital camera is used to take infrared images of the hot slab. Data is read from the camera at a preset frequency.

Figure 1. Online width measurement system for hot slabs.(FU JianXun et al. 2011(b))

Then, the graphics module creates images of the hot slab according to color aberration, and saves the images as files. The accuracy of the online system is 1 mm. A photograph of the system is shown in Figure 1.

2.3. RAS and RUB investigation

Table 1 lists the RAS and RUB values obtained for five companies. The data in the right column is from a handbook (XIONG Yi-gang, 1994). The RAS values range from 0.47% to 2.16%, with most being higher than the handbook data. The linear shrinkage of carbon steel from the initial shell to the cooled slab is 2.5%. The RUB values range from 0.34% to 2.03%, which is the result that the linear shrinkage subtracting the RAS. In general, the width of a slab is smaller than the top width of a mold. Broadening may overcome shrinkage under certain operating conditions for some particular grades of steel.

The width of a cooled slab is larger than the ultimate width when broadening exists. To obtain a slab with the desired dimensions, the top and bottom widths of the mold must be reset. Therefore, the measured width (W) could replace the ultimate width (T). The RAS of a slab can thus be set by changing the values of the top and bottom widths of the mold. Then compare these values with the linear shrinkage of each steel grade, and it could consequently be found out whether the slab broadening exists and the approximate range of it could also be derived.

	CompanyA	Company B	Company C	Company D	Company E	Handbook
RAS (%)	0.47~0.54	1.81	1.93~2.16	1.70~1.90	1.10 ~2.11	2.1
RUB (%)	1.96~2.03	0.69	0.34~0.57	0.60~0.80	0.39~1.40	0.4

Table 1. RAS and RUB values at various manufactures (FU JianXun et al. 2010(a))

The data show that slab broadening is common in continuous casting. The slab width is the result of shrinkage and broadening. The linear shrinkage of a carbon steel is about 2.5%, which is slightly larger than the slab broadening.

2.4. Mechanics calculations (FU JianXun et al.2011(a))

In the secondary cooling zone, the slab has to release sensible heat and latent heat to avoid complete solidification and to maintain the surface temperature according to the technical requirements of the metallurgy process. In this zone, the stress and strain of the slab are the result of mechanical action and thermal effects (S. Kobayashi et al,1988). Some parts of the slab may have a low temperature, which causes thermal stress in the secondary cooling zone. The thermal stress of the slab in the secondary cooling zone is small enough to be ignored compared to the stress caused by the bulging and the roller disalignment. Thus, mechanical stresses, includes the bending stress, straightening stress, roller-misalignment stress, the stress of rollers acting on the slab, and the static pressure of molten steel, determine the degree of slab broadening.

The bulging stress of a slab is defined as (Sheng Y et al ,1993) :

$$\delta = \frac{pl^4}{32E_xS^3} + \frac{pl^4}{32E_xS^3}(1\text{sqrt(t)}), \tag{3}$$

where E_x is the equivalent elastic modular ratio, expressed as:(Sheng Y et al ,1993)

$$E_{\mathrm{x}} = \frac{T_{So} - T_m}{T_{so} - 100} \times 10^6, \tag{4}$$

The stress of bending and straightening is expressed as:(Lei H et al ,2007)

$$\varepsilon_i = \left(\frac{D_s}{2} - S_i \right) \left(\frac{1}{Ri - \frac{D_s}{2}} - \frac{1}{R_{i+1} - \frac{D_s}{2}} \right) \times 100\%, \tag{5}$$

The stress of disalignment is expressed as: (Chen J,1990)

$$\varepsilon_{\mathrm{q}} = \frac{300 s_i \delta}{l^2} \times 100\%, \tag{6}$$

The values of these stresses calculated for the Q235 slab are listed in Tables 2 and 3. The calculations were based on the parameters of the continuous casters of Maanshan Iron and Steel Co. Ltd. A casting speed of 0.0167 m·s-1 was used. The bending zone of the continuous caster is at the 10th~15th rollers of the 2nd segments, and the straightening zone is at the 60th~65th rollers of the 9th segments. A negative stress indicates that a pushing stress acts on the contact surface between the slab and rollers whereas a positive stress indicates a tensile stress acting on the contact surface.

Roller ID	Slab shell thickness (10^{-2} m)	Casting speed ($m \cdot s^{-1}$)	Bulging (10^{-2} m)	Bulging strain(%)	Disalignment strain(%)	Bending strain(%)
10	4.10	0.0167	0.101	0.115	0.0128	-0.0011
11	4.28	0.0167	0.097	0.115	0.0134	-0.0011
12	4.45	0.0167	0.093	0.115	0.0139	-0.0012
13	4.62	0.0167	0.090	0.115	0.0144	-0.0013
14	4.78	0.0167	0.087	0.115	0.0149	-0.0011
15	4.93	0.0167	0.084	0.115	0.0154	-0.0010

Table 2. Comparison of slab stresses in the bending zone(FU JianXun et al.2011(a))

Roller ID	Slab shell thickness (10^{-2} m)	Casting speed ($m \cdot s^{-1}$)	Bulging (10^{-2} m)	Bulging strain(%)	Disalignment strain(%)	Bending strain (%)
60	10.4	0.0167	0.14	0.196	0.0160	0.0160
61	10.5	0.0167	0.09	0.152	0.0197	0.0197
62	10.6	0.0167	0.08	0.149	0.0198	0.0198
63	10.7	0.0167	0.08	0.147	0.0200	0.0200

Roller ID	Slab shell thickness (10^{-2} m)	Casting speed ($m \cdot s^{-1}$)	Bulging (10^{-2} m)	Bulging strain(%)	Disalignment strain(%)	Bending strain (%)
64	10.8	0.0167	0.08	0.145	0.0202	0.0202
65	10.9	0.0167	0.08	0.142	0.0203	0.0203

Table 3. Comparison of slab stresses in the straightening zone(FU JianXun et al.2011(a))

Tables 2 and 3 reveal that the bending, straightening, and disalignment stresses are far lower than the stress of bulging. Therefore, the stresses of bending, straightening, and disalignment do not cause the broadening of a slab.

3. Model and parameters

3.1. Finite element model

Building a satisfactory three-dimensional (3D) finite element model for the numerical simulation of continuous casting in the secondary cooling zone is quite complex. Thus, to simplify the problem, the following assumptions are made, as in our previous work((FU JianXun et al. 2010(b-c); 2011(b)):

1. The bending and straightening effects of the slab are ignored, and the slab is considered to be a linear object.
2. In the simulations, time, space, the characteristics of steel, and the temperature field in the slab are continuous, and the effects of the initial mechanical conditions of the slab on the deformation are ignored. The continuous caster in the secondary cooling zone is divided into several stages.
3. Because of symmetry, 1/4 of the slab and rollers on one side is used for the calculation.
4. The slab is deformable, the rollers are stiff, and the gap between rollers is variable. The calculation boundaries are placed at the rollers.

Based on these assumptions, the thermal-mechanical coupled model of the whole secondary cooling zone is divided into 6 independent sub-models for calculation. The 15 segments of the secondary cooling zone are divided into 6 groups. The first 5 groups each contain 2 segments; the remaining 5 segments make up the last group as a completely solidified slab. A 2-m slab is used for the simulation. The slab goes through the roll arrangement at a given speed. The simulation is performed continuously from the first group to the last group, and the results of a group of rollers are taken as the initial inputs for the subsequent group.

Eight-node isoparametric elements are used for the geometric discretization of the computational domain in the model. The slab comprises 4500 elements and 5250 nodes. Figure 2 shows the finite element models of the rollers and the slab in the caster. Figure 3(a) shows the rollers and the slab in the 3rd independent sub-model. Figure 3(b) shows the 6th independent sub-model.

Due to the symmetry of the slab in the width direction, one half of the slab was simulated. The grid units at the start plane of the slab move forward at a given speed. The static

pressure of molten steel is taken as a mechanical boundary condition. The boundary is applied to the solidifying front of the slab, which is defined as the position with zero-strength temperature (ZST). Considering the effects of solidification-induced segregation and solid fraction (*f*s), the temperature of the units is the ZST where *f*s is equal to 0.8, and the units are considered a solidified shell where *f*s $\geq$ 0.8. T_{80} denotes the temperature at the boundary between the solid phase and the liquid phase (T_{80}=ZST). Static pressure acts on the units where the temperature is higher than T_{80}. The boundary conditions of heat transfer and contact are also applied to the model.

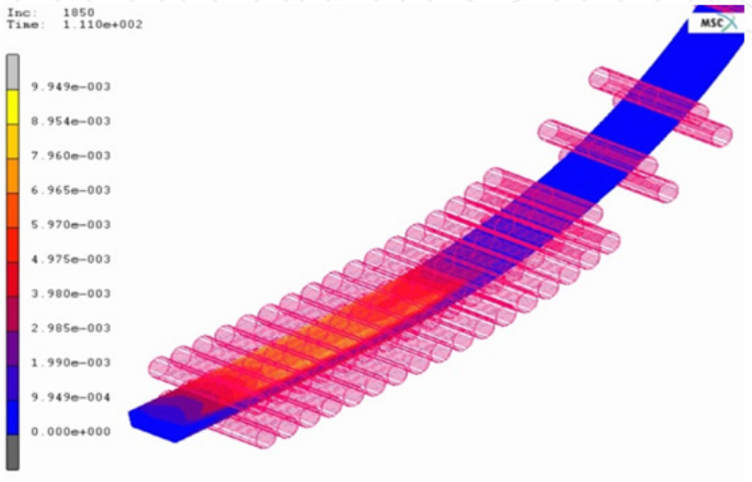

Figure 2. Finite element model of all the rollers and the slab (FU JianXun et al. 2011(b))

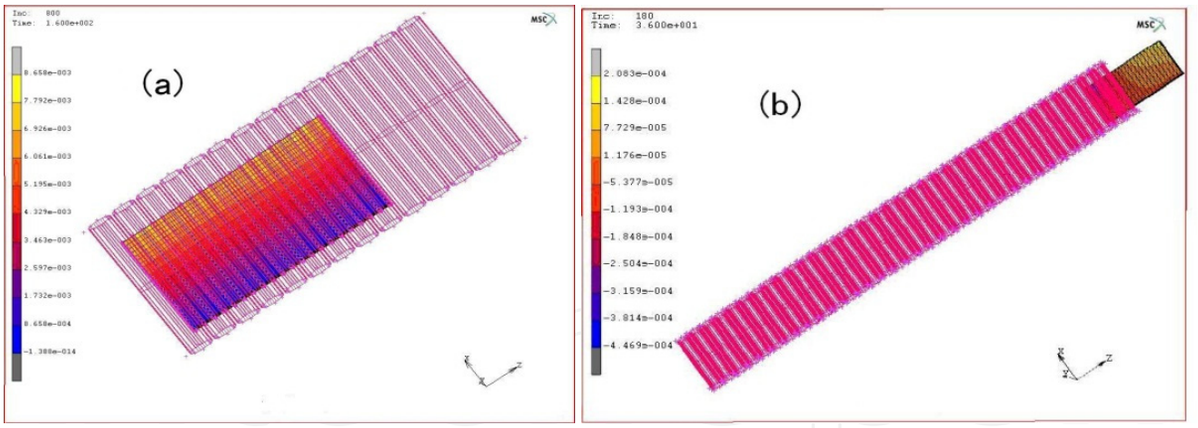

Figure 3. Finite element models of (a) the third group of rollers and the slab (b)the sixth group of rollers(FU JianXun et al. 2010(c))

3.2. Constitutive equations

The key factors that determine the accuracy of a model for analyzing the stress in a slab are included in the constitutive equation of the slab. These factors are heat transfer, mechanical load, stress relaxation, and plastic strain, all of which are time-dependent. The constitutive equation of steel at high temperature, which determines the accuracy of numeric simulations, is expressed as:

$$\varepsilon_{ij} = \varepsilon_{ij}^{e} + \varepsilon_{ij}^{ie} + \varepsilon_{ij}^{T}. \tag{7}$$

where:

ε_{ij} is the total strain;
ε_{ij}^{e} is the elastic strain;
ε_{ij}^{ie} is the non-elastic strain;
ε_{ij}^{T} is the thermal strain, and ij is the strain tensor.

The non-elastic strain ε_{ij}^{ie} is composed of time-independent inelastic strain and time-dependent creep deformation. A viscoelastic-plastic model is used to describe the solidifying behavior of the slab under the conditions of continuous casting, which is expressed as: (Chen J,1990)

$$\dot{\varepsilon}_{ij}^{ie} = f(\sigma_{ij}, T, \varepsilon_{ij}^{ie}). \tag{8}$$

where: $\dot{\varepsilon}_{ij}^{ie}$ is the non-elastic strain ratio; σ_{ij} is the stress; and T is the temperature.

This equation indicates that the non-elastic strain ratio is a function of the stress, temperature, and non-elastic strain.

The constitutive equation of time-dependent plastic deformation is used to describe the stress of carbon steel under various temperatures and strain ratios; it is expressed as: (S. Kobayashi et al.,1988)

$$\begin{cases} \dot{\bar{\varepsilon}}_P = \mathrm{A}\exp(-\mathrm{Q}/\mathrm{R}T)[\sinh(\beta K)]^{1/m}, \\ \bar{\sigma} = K \cdot (\bar{\varepsilon}_{\mathrm{p}})^{n}, \end{cases}. \tag{9}$$

where:

$\dot{\bar{\varepsilon}}_P$ is the equivalent plastic strain ratio;
R is the gas constant;
Q is the activation energy of deformation;
σ is the equivalent stress;
$\bar{\varepsilon}_P$ is the equivalent plastic strain;
K is the strength factor;
n is the factor of hardening; and A, β, m are constants.

When carbon steel becomes plastic, strain hardening is observed. The coefficient of strain hardening can be obtained from the following equation:

$$H = K \cdot n \cdot (\bar{\varepsilon}_{\mathrm{p}})^{n-1}. \tag{10}$$

In this work, the user program includes the strain hardening coefficient in the elastic-plastic model of the MSC.Marc solver to describe the viscoelastic-plastic behavior of the cast slab under high temperature. The work hardening of carbon steel is described by the equations given by Sorimachi and Brimacombe (K. Sorimachi et al.,1977);

$$K_1 / E = 0.13\exp(-0.023\theta), \tag{11}$$

$$K_2 / E = \begin{cases} 0.045 - 3.87 \times 10^{-5}\theta \ , \ \theta < 1050^{\circ}C \\ 0.385 \cdot \exp(-0.00422\theta) \ , \ \theta \geq 1050^{\circ}C \end{cases}, \tag{12}$$

$$K_3 / E = \begin{cases} 0.0197 - 1.68 \times 10^{-5}\theta \ , \ \theta < 1050^{\circ}C \\ 0.0226\exp(-0.00223\theta) \ , \ \theta \geq 1050^{\circ}C \end{cases}, \tag{13}$$

where: E is the elastic modulus; K_1~K_3 are factors of hardening; Θ is the temperature (°C).

Equations (11)~(13) are applied when the strain is smaller than 0.01~0.02, and greater than 0.02, respectively. The factors of hardening are incorporated into the elastic-plastic model in the software package Marc by the user programs.

3.3. Parameters

All simulation parameters are taken from the technological parameters of the #2 continuous caster (SMS-Demag) of Maanshan Iron and Steel Co. Ltd. The parameters of the continuous caster are listed in Table 4.

Segment No.	Shrinkage between rollers (mm)	Slab thickness (m)	Roller diameter(m)	Slit width between rollers (m)	Distance from meniscus (m)
1-2	0.20/0.46	0.2375	0.200	0.240	0-4.374
3-4	0.46/0.46	0.2370	0.245	0.284	4.374-8.388
5-6	0.46/0.44	0.2362	0.255	0.297	8.388-12.592
7-8	0.44/0.44	0.2354	0.265	0.310	12.592-16.992
9-10	0/0.30	0.2346	0.283	0.322	16.992-21.254
11-15	0.30/0.30	0.2343	0.300	0.335	21.254-33.249

Table 4. Parameters of the slab and caster at various segments

Casting temperature: T=1533 °C;
Liquidus temperature T_l=1513 °C;
Solidus temperature T_s =1446.0 °C;
T_{80} = 1459.6 °C;
Environmental temperature: 25 °C;
Roller temperature: 100 °C;
Coefficient of contact heat transfer: 25.0 W/(m·K) (Y. S. Xi and H. H. Chen,2001) ;
Coefficient of fraction: 0.3; Distance tolerance: 0.01 (Y. S. Xi and H. H. Chen,2001).

When the casting speed is in the range of 1.0~1.2 m/min, the SMS-Demag casting machine uses a fixed cooling water intensity in the secondary cooling zone. The parameters of the SPHC steel and Q235 steel are listed in Table 5.

Steel	C (%)	S i(%)	M_n(%)	P(%)	S(%)	Al(%)	T_l(°C)	T_s(°C)
SPHC	0.05	0.05	0.20	≦0.02	≦0.012	0.03	1528.9	1493.0
Q235	0.18	0.20	0.40	≦0.025	≦0.022		1517.0	1446.0

Table 5. Compositions of SPHC steel and Q235 steel

The coefficient of thermal expansion, Young's modulus of elasticity, and Poisson's ratio of the steel as functions of temperature are required for simulation. The elastic modulus of carbon steel for various temperatures during continuous casting is given in equations (14) and (15).(Ueshima Y et al; 1986, I.Ohnaka,1986)

$$\begin{cases} E = (347.6525\text{-}0.350305*\mathrm{T}) * 10^9 \quad , \ T < 900 \ , \\ E = (968 - 2.33 * T + (1.9 * 10^{-3}) * \mathrm{T}^2 - (5.18 * 10^{-7}) * T^3) * 10^9 \quad , \ Ts > T \geq 900, \end{cases} \tag{14}$$

$$E = \frac{(f_S - f_{ZST}) \cdot E_S + (1 - f_S) \cdot E_{ZST}}{1 - f_{ZST}}, \quad T_{80} > T > T_S (f_{ZST} \leq f_S \leq 1), \tag{15}$$

When E=E(Ts) and Ezst=E(Tzst), Ezst takes a small non-zero value in order to restrain the deviatoric stress in the liquid phase region to maintain hydrostatic pressure. When the temperature is lower than Ts, the elastic modulus is expressed by (14); when it is higher than T_s, it is expressed by (15).

When the temperature is lower than Ts, Poisson's ratio can be defined as equation (14); when the temperature is higher than T_s, with decreasing f_s, Poisson's ratio gradually increases from the value at Ts to a certain value which is close to 0.5; it remains at this value above ZST, as expressed by equations (16) and (17). (Uehara M et al.,1986)

$$\nu = \frac{(f_s - f_{ZST}) \cdot \nu_s + (1 - f_s) \cdot \nu_{ZST}}{1 - f_{ZST}}, \ \mathrm{T} > \mathrm{T_L} \ \left(f_{ZST} \leq f_S \leq 1\right), \tag{16}$$

$$\nu = \nu_{ZST}, \quad T \geq T_{80} \quad , \quad (f_S \geq f_{ZST}). \tag{17}$$

Where f_{ZST} is the solid phase ratio at ZST, often taken as 0.80. ν_{ZST} is the Poisson's ratio at ZST; it is very close to 0.5. The Poisson's ratio of the steel for various temperatures is shown in Figure 4(a). The coefficient of thermal expansion values of Q235 and SPHC are taken from the local measurement results shown in Figure 4(b).

4. Effects of casting speed on slab broadening (Jian-Xun Fu et al , 2011b)

4.1. Numerical simulation

By tracing one node of the slab at the side-face and recording its width, the width of the slab at various positions in the secondary cooling zone can be obtained. The RUB can then be derived from the simulated width of the slab. The simulated RUB values of Q235 and SPHC steels at three casting speeds are shown in Figure 5(a) and (b), respectively.

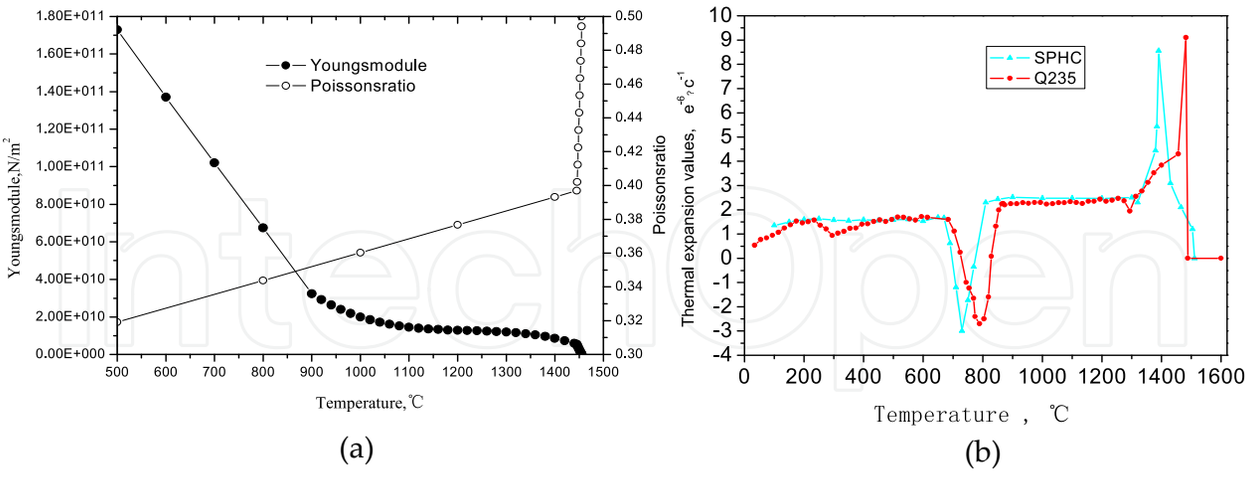

Figure 4. (a) Young's modulus of elasticity and Poisson's ratio of Q235 steel for various temperatures; (b)Coefficient of thermal expansion of Q235 and SPHC. (Jian-Xun Fu et al , 2011b)

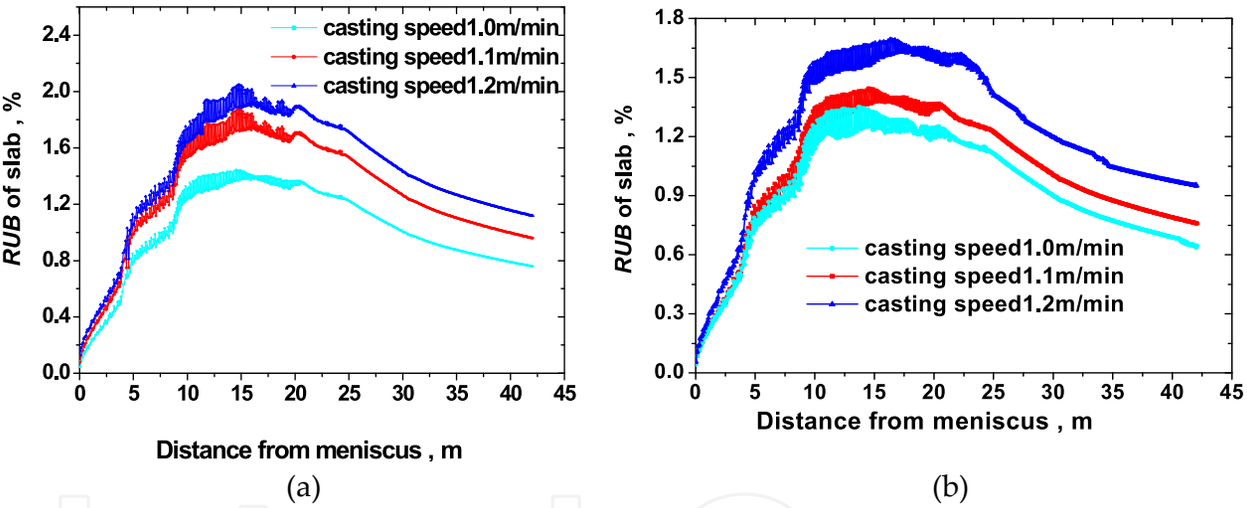

Figure 5. (a) RUB values versus distance from meniscus of a Q235 steel;.(b) RUB values versus distance from meniscus of a SPHC steel at three casting speeds. (FU JianXun et al. 2011(b))

Slab broadening for Q235 and SPHC steels at three casting speeds shows similar characteristics. The values of the RUB at the three casting speeds are all positive in the whole secondary cooling zone, which means that slab broadening existed for Q235 and SPHC steels at these speeds. The RUB changed from one segment to another for the first five segments. The RUB increased and then gradually decreased after reaching its maximum at the fifth and sixth segments. Near the tenth segment, the RUB decreased smoothly; the slab became completely solidified at this location.

The simulations of Q235 and SPHC steels produced similar results. The RUB increased with increasing casting speed. For Q235 steel, when the casting speeds were 1.0, 1.1, and 1.2 m/min, the maximum RUB values were 1.44%, 1.88%, and 2.04 %, respectively, and the RUB

values at the exit of the caster were 0.76%, 0.96%, and 1.14%, respectively. For SPHC steel, when the casting speeds were 1.0, 1.1, and 1.2 m/min, the maximum RUB values were 1.34%, 1.44%, and 1.69%, respectively, and the RUB values at the exit of the caster were 0.64%, 0.76%, and 0.95%, respectively.

Slab broadening is closely correlated with casting speed, which may be due to the slab's temperature changing with casting speed. When the casting speed increased, the liquid core length and temperature of the slab both increased. With increasing temperature of the slab, the high-temperature mechanical properties of the slab changed; ductility increased and the strength and resistance to external pressure decreased, increasing the RUB.

With increasing casting speed, a given cross section of the slab takes up the same amount of space. At 25 m away from the meniscus, the surface temperature in the wide face at a casting speed of 1.2m/min is 11.6 °C and 21.7 °C higher on average than those at casting speeds of 1.1 and 1.0 m/min, respectively (see Figure 6). Under a given set of conditions, increasing the casting speed increases production. However, high casting speed can lead to slab broadening.

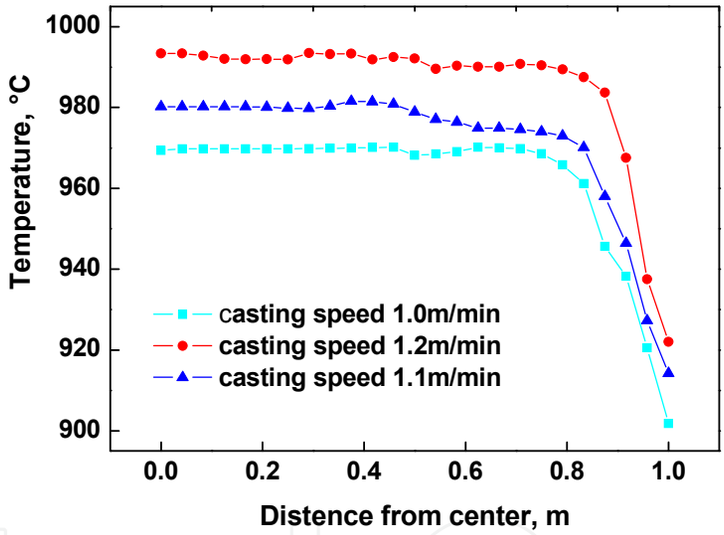

Figure 6. Surface temperature on the slab at various positions.(FU JianXun et al. 2011(b))

4.2. Verification of simulation results

For continuous caster #2 at Maanshan Iron and Steel Co. Ltd., the slab widths of two steel grades were tracked online at the exit of the caster (the end of the 15th segment); the slab width was measured once per minute. For each grade of steel, measurements were taken for more than 70 minutes. The data are shown in Figures 7(a), and (b), respectively.

Figure 7(a) shows the slab width and the RUB of SPHC steel at various moments. Slab broadening can be clearly seen. The RUB of SPHC steel ranges from 1.4% to 2.4%, with an average of 1.96%. The average RUB is greater than the ratio of linear shrinkage, indicating that the width of the slab after cooling was greater than the top width of the mold. This result shows that slab broadening occurred in the secondary cooling zone.

The slab width changed smoothly except from 45 to 55 min, during which time a sharp trough appears on the RUB curve. In the initial 6 minutes of this period, the RUB decreased to 1.4% from 2.25%, and in the following 4 minutes, the RUB increased to 2.1% from 1.4%. This trough was caused by the changing of the tundish, during which the casting speed decreased sharply, and then quickly recovered to normal; i.e., the change in casting speed caused the change in slab broadening.

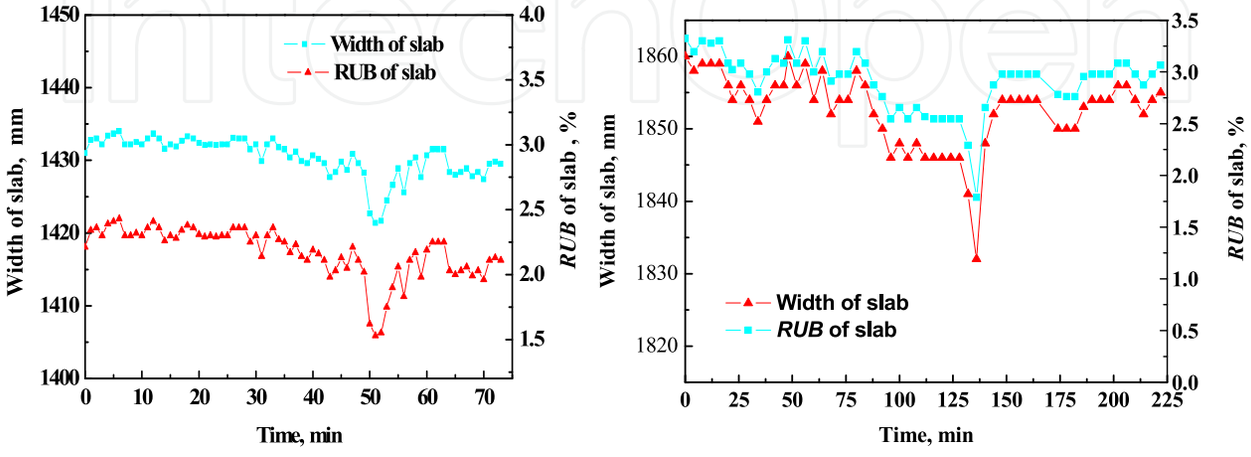

Figure 7. (a) Width of slab and RUB for SPHC steel at various moments; (b) Width and RUB for Q235 steel at various moments. (FU JianXun et al. 2011(b))

Figure 7(b) shows the slab width and the RUB for Q235 steel at various times. The RUB for Q235 steel ranges from 0.77% to 2.91%, with an average of 2.04%. There are five sharp corners on the RUB curve for Q235 steel. By comparing the curve with the production process of Q235, it was found that each sharp corner corresponds to an unsteady production stage. The biggest one corresponds to the changing of the tundish, the last one corresponds to the end of casting, and the remaining three correspond to the changing of ladles.

Figure 8 shows the relationship between the RUB and the casting speed for Q235 steel. The shapes of the RUB curve and the casting speed curve are very similar. When the tundish was changed, the casting speed decreased to 0.5 m/min over a 10-minute period and then recovered to normal in 5 minutes; this change formed a sharp trough in the casting speed curve. At nearly the same time, the RUB decreased to 1.91% from 0.77% in 10 minutes and then increased to 2.1% in 5 minutes, producing a sharp trough in the curve. When the ladle was changed, a similar change happened. When the casting speed was maintained at 1.0 m/min, the RUB remained stable at about 2.0%. The RUB is thus closely correlated with casting speed.

There is a small lag between the RUB curve and the casting speed curve in Figure 12. The change in casting speed curve occurred earlier than that in the RUB curve. For example, the casting speed curve exhibits a sharp trough at about 100 minutes; a sharp trough appears in the RUB curve at about 110 minutes. Comparing Figure 7 and Figure 8, it can be seen that the simulation results generally agree with the industrial measurement results.

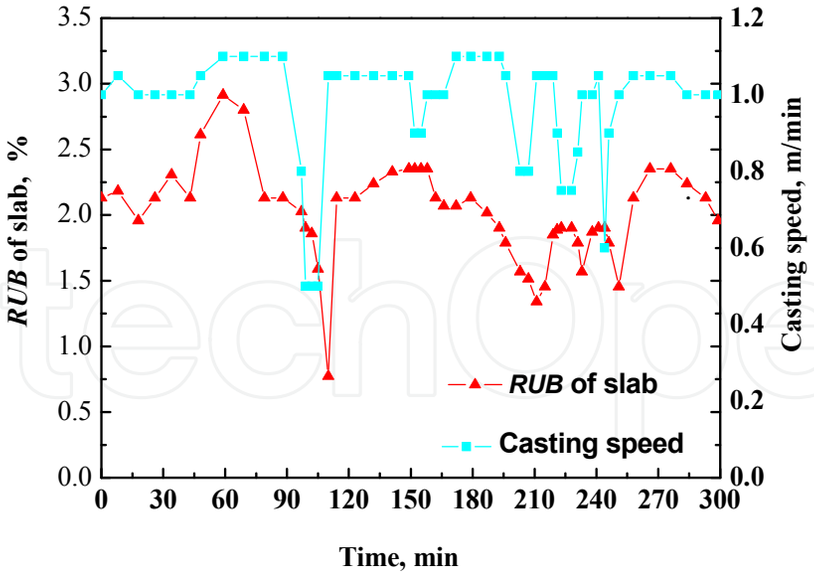

Figure 8. Relationship between the RUB and casting speed. (FU JianXun et al. 2011(b))

5. Effects of width and thickness on slab broadening (FU JianXun et al. 2010(b))

5.1. Numerical simulation

One node of the slab was traced and the width was recorded at various positions of the secondary cooling zone. The RUB was derived from the calculated width of the slab.

The calculated RUB of Q235 steel slab with a cross section 2000 mm × 230 mm at speed of 1.0m/min is shown in Figure 9(a). The RUB changes from one segment to another; its value is over 0 throughout the secondary cooling zone, indicating slab broadening. The RUB increases in the first five segments, and then drops down gradually after reaching its maximum in the sixth segment. In the sixth segment, the width of the slab reaches its maximum with a large fluctuation due to the bulging of the slab in the direction of thickness. Figure 9(b) shows the simulated deformation of the slab in this direction. The shell of the slab has low yield strength and high plasticity; thus, the slab at the points contacting the rollers is depressed and bulges at the slit between the two rollers. Similar to the periodicity of bulging, the width of the slab fluctuates periodically.

The simulated broadening and bulging of the slab in the sixth segment are shown in Figure 10. There is an obvious correlation between broadening in the width direction and bulging in the thickness direction. The position in the slab where the smallest bulging is observed has the greatest broadening. This is due to the depression of slab in the thickness direction contributing to slab broadening in the width direction.

5.2. Effects of slab width on broadening (FU JianXun et al. 2010(b))

230-mm-thick slabs of Q235 with various widths were simulated at a casting speed of 1.0 m/min. The RUB values for various segments are shown in Figure 11. It shows that the

simulated RUB of slab slightly increases with the increase of width. The maximum values are 1.27 %, 1.36 %, and 1.44 %, respectively. The RUBs at the exit of caster are 0.63 %, 0.70 %, and 0.76 %, respectively. There is no obvious increase of RUB for slabs with increasing the width, but the increase of broadened size is noticeable. In conclusion, slabs with great width have great broadening.

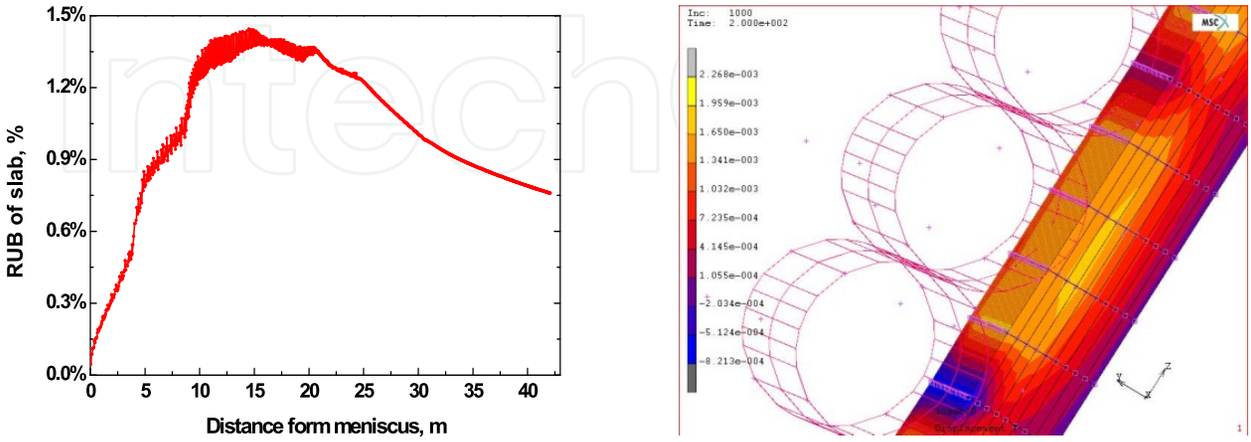

Figure 9. (a) Calculated RUB of Q235 steel in the secondary cooling zone; (b)Calculated deformation of slab between rollers. (FU JianXun et al. 2010(b))

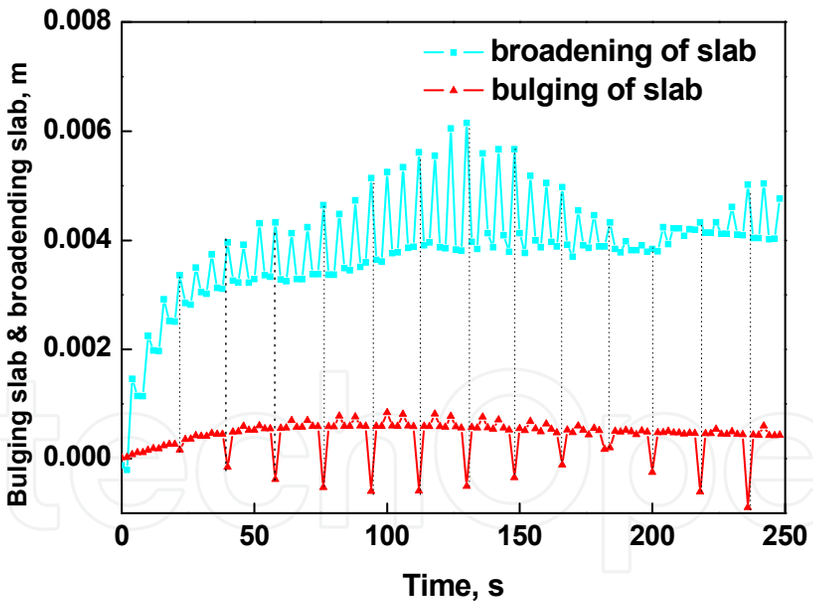

Figure 10. Broadening and bulging of slab in the sixth segment. (FU JianXun et al. 2010(b))

Under the same conditions, the wide slab has greater broadening than narrow slab because of compound effects of temperature and stress. Compared with wide slab, narrow slab has a larger range for heat flow distribution and hence the greater equivalent von Mises stress. But the wider slab has more enthalpy to be removed. So in the same position of caster, the narrow slab has higher yield strength and lower plasticity, and the solidified shell is able to resist great stress.

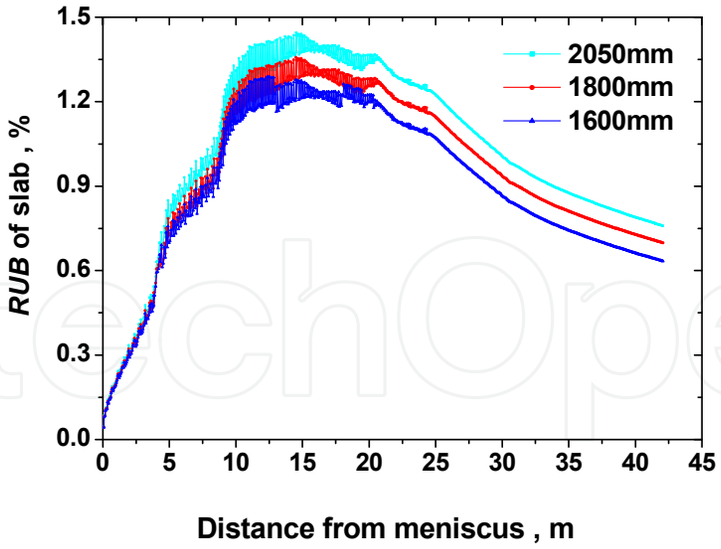

Figure 11. Calculated RUB values for slabs of various widths . (FU JianXun et al. 2010(b))

5.3. Effects of slab thickness on broadening

To study the effect of slab thickness on broadening, 2050-mm-thick Q235 slabs with thicknesses of 230 and 250 mm, respectively, were simulated at a casting speed of 1.0 m/min; the results are shown in Figure 12.

The calculated broadening values for the two slabs are slightly different. The maximum RUB values are 1.4% and 1.38% for 250- and 230-mm-thick slabs, respectively. The RUB values are 0.74% and 0.71% at the exit of the continuous caster, respectively. The difference of broadening is just 0.6 mm between the two slabs. This is because the bulging changes little with increasing thickness.

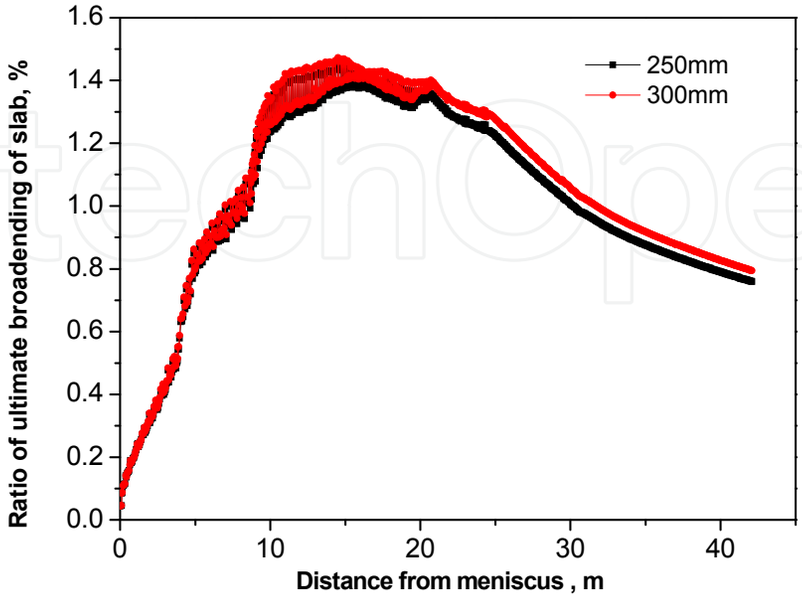

Figure 12. Calculated RUB with different thicknesses. (FU JianXun et al. 2010(b))

5.4. Verification of simulation results

To verify the obtained simulation results, the slab broadening cast on the #2 caster in Maanshan Iron and Steel Co. Ltd was measured. The online measuring system was designed to measure the width of the slab. The digital camera was fixed above the exit of the caster. Q235 steel was used for the experiments. The parameters of the continuous caster and measured results are listed in Table 6.

The online measured RUB values are greater than the simulation results for all the experimental slabs. This is because the preset width of a cold slab in the experiments was the upper width of the mold. The upper width is always greater than the defined width. For the slab with a preset width of 2050 mm, the upper width of the mold is 2081.3 mm (a broadening of 1.56%). With this difference taken into account, the experimental results well agree with those of the simulation.

Defined width (mm)	Upper width (mm)	Lower width of mold (mm)	Measured width (mm)	Measured RUB (%)	Measured broadening (mm)	Calculated broadening (mm)	Deviation rate (%)
1600	1623.8	1610.4	1630.4	1.90	6.6	7.04	6.7
1850	1877.7	1867.3	1885.9	1.94	8.2	9.25	12.8
2050	2081.3	2067.5	2091.4	2.02	10.3	11.69	13.5

Note: the measured broadening of the slab is the difference between the measured width of the slab and the upper width of the mold, and the calculated broadening of the slab is that between the calculated width and the defined width.

Table 6. Measured and calculated widths of slabs

6. Analysis of slab broadening (FU JianXun et al.2011(a))

6.1. Change of mold size

The slabs broaden in width, which varies with the operating parameters of steel produced. The statistical data of 76 taper samples of the mold revealed that the change is very small for the taper of the mold. The average change of a one-sided taper was 0.37 mm, and only a few samples had changes of 1~2 mm. The slight change of the taper is due to metering errors, wear, and deformation. Slab broadening is thus independent of the mold size.

6.2. Exception of equipment or operating parameters

The secondary cooling process is the most important procedure in continuous casting. The temperature field of the slab was checked with the data provided by the producer of the caster. A good agreement was found, indicating that the caster worked well in the secondary cooling process. The monitoring records obtained in a controlled room also reveal that the caster worked well. However, the width of the produced slabs exhibited obvious

broadening during the process. It is thus concluded that slab broadening is independent of exceptions of equipment or operating parameters.

6.3. Soft reduction

Soft reduction may strengthen slab broadening and even cause side bulging. For SPHC and Q235 steels, the slabs were broadened in the process of continuous casting with soft reduction set to 0.5~2.5 mm. The broadening width ranges are 2~19 mm and 2~8 mm for SPHC and Q235 steels, respectively. The ratios of broadening are 0.1%~1.46% and 0.15%~0.62% for SPHC and Q235 steels, respectively. Therefore, soft reduction contributes to slab broadening, but is not the main cause.

6.4. Contraction of roll gap

For the continuous caster #2 in Maanshan Iron and Steel Co. Ltd, the ultimate thickness of a produced slab is 230 mm, and the bottom thickness of the mold is 237.5 mm. With a casting speed of 1.1 m/min, the molten steel completely solidifies at the start of the 11th sector where the thickness of the slab is 234.3 mm and the roll gap contraction is 3.2 mm. In this zone, the linear shrinkage ratio is 0.5%~0.7% (1.2~1.7 mm) due to the drop of temperature. Without the contribution of the temperature drop, the roll gap contraction is 1.5~2.0 mm. This amount of shrinkage equals soft reduction of medium or light scale. The roll gap contraction is uniformly distributed. The roll gap contraction acts on the slab and affects the fluctuation of the liquid level of molten steel. However, the slab broadening is far less than that induced by soft reduction. So roll gap contraction is not the main cause of broadening.

6.5. Summary

The static pressure of the molten steel core and the force of the driving rollers may be the main cause of slab broadening.

When there is no support on the narrow face of a slab, the slab deforms in the width direction under the static pressure of molten steel. The high-temperature mechanical properties of the slab are worse than those under normal temperature(Lei H et al,2007; Chen J,1990; S. Kobayashi et al,1988). The slab has good ductility under high temperature and is unable to resist the static pressure of molten steel in the width direction. Therefore, the slab greatly deforms at the edges, and thus the width is broadened. Previous studies found that the hardness of the solidified shell and the ability to resist the static pressure of molten steel are determined by the thickness of the shell and the formation of ferrite-austenite with a dual phase.(Mizukami H et al,1977; Uehara M et al, 1986; Ramacciotti A,1988)

The shell of the slab is clamped under the pressure of the driving roll cylinders so that it moves forward with the rotation of the driving rollers. The solidifying and soft slab is extended and broadens under the pressure of the driving rollers when passing through

the cast-rolling segment. The degree of extension and broadening increases with casting speed.

6.6. Creep deformation

The forces acting on the slab shell in the secondary cooling zone can be modeled as the bending of a rectangular thin plate under loading (i.e., static pressure of molten steel). One segment of the slab along the strand direction is taken to build the model. In the model, the slab is a rectangular thin plate fixedly supported along two sides and simply supported along the other two sides. In addition, the thin plate is subjected to lateral loads, and the temperature field linearly changes in the thickness direction of the slab. Because the width of the slab is much greater than the gap between the rollers, the effects of the slab boundary on the internal side of the slab can be ignored according to the Saint-Venant principle. According to plate theory, the slab shell is viscoelastic at high temperature, and the stress and deformation satisfy the Maxwell creep law. As shown in Figure 13.

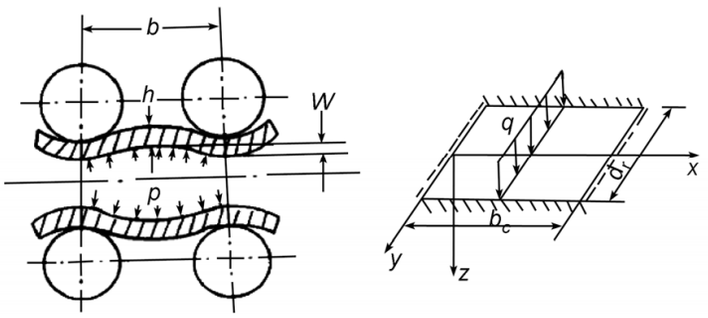

Figure 13. Model of slab shell and the force model of slab creep. (Sun J et al,1996)

In the secondary cooling zone, the total stress equals the sum of elastic strain and creep strain, when the slab shell creepily bends under the static pressure of molten steel. The elastic strain changes little with time. The elastic deflection is expressed as: (Sun J et al,1996):

$$W_e(x,y) = W_{qe} + W_{Te} = \frac{4q\alpha^4}{\pi^5 D}\sum_{i=1,3\ldots}^{\infty}\frac{1}{m^5}\times$$
$$\left(1-\frac{\alpha_m ch\alpha_m + sh\alpha_m}{\alpha_m + sh\alpha_m ch\alpha_m}ch\frac{2\alpha_m}{b}y + \frac{\sigma_m sh\alpha_m}{\alpha_m + sh\alpha_m ch\alpha_m}\cdot\frac{2y}{b}sh\frac{2\alpha}{b}y\right) \quad (18)$$
$$\times\sin\frac{m\pi}{\alpha}x + \frac{48\alpha a T_0}{\pi^3 h^3(1-2\gamma)(1-\gamma)}\times\sum_{i=1,3\ldots}^{\infty}(1-\frac{ch\frac{2\alpha_m}{b}y}{ch\alpha_m})\sin\frac{m\pi}{a}x.$$

where: $T_0 = \int_{-h/2}^{h/2} T(z)\cdot z\cdot \mathrm{d}z$.

The expression of elastic deflection has the series of hyperbolic function, and converges rapidly, thus setting m=1 is sufficiently accurate for calculation. Using equation (18) and the Cauchy equation, the creep deformation of slab shell on the narrow side can be derived as:

$$\begin{cases} \varepsilon_{xe} = -\dfrac{\partial^2 W_e}{\partial x^2} z, \\ \varepsilon_{ye} = -\dfrac{\partial^2 W_e}{\partial y^2} z, \\ \gamma_{xye} = -\dfrac{\partial^2 W_e}{\partial x \partial y} z. \end{cases} \tag{19}$$

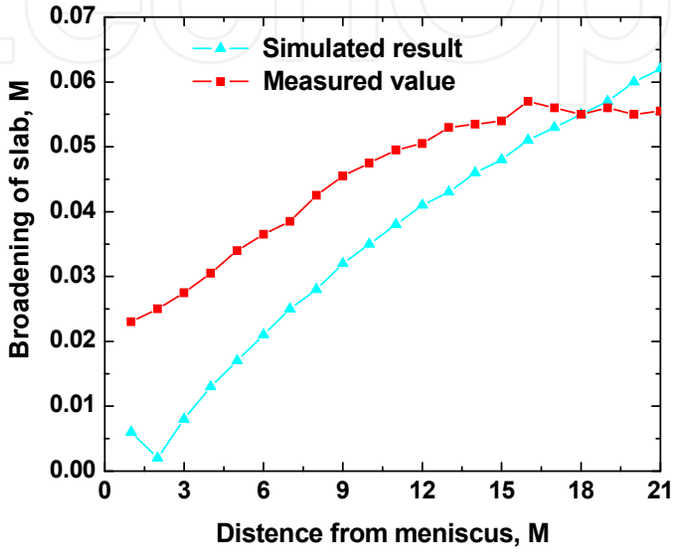

Figure 14. Comparion of calculated and measured side creep results. (FU JianXun et al.2011(a))

The amount of creep deformation for the narrow side of the slab was calculated using Matlab software; the results are shown in Figure 14. The figure also shows the measured results from the experiments of a stagnant slab. The agreement between the calculated results from the Maxwell model and the measured results illustrates that the Maxwell model is able to reveal deformation behavior at high temperature.

6.7. Industrial experiments of stagnant slab (FU JianXun et al.2011(a))

If the static pressure of molten steel is the main reason for the broadening of a slab, the broadening must happen at the forepart of the continuous caster where the slab has a high temperature and a thin shell. If the stress of the rollers is the main reason for broadening, the broadening must happen at the middle part of the continuous caster, specifically the position near the completely solidified zone. Because the molten steel is fluidic before this part(Lin Q Y et al ,2004), decreasing the roller gap does not broaden the slab.

Since the continuous caster is a vertical bow type, it is very dangerous to keep close to it, and thus it is impossible to measure the width of the slab directly. Therefore, when the caster stopped to for the tundish replacement, the width of the stagnant slab was measured to determine where slab broadening happens. When the tundish is to be replaced, the casting speed gradually slows down to zero. This process takes about 4-5 min to form a

stagnant slab, which is cooled down continuously by secondary cooling water. The slab in the continuous caster is composed of three parts:

1. For the fully solidified part during casting, the slab broadening is the sum of broadening of the molten steel core.
2. For the part solidified during the stopping period, because it reveals the slab broadening at specific position, and corresponds to the real broadening amount of slab, this part is focused on in our experiments.
3. For the unsolidified part until restarting the casting, the slab broadening continues during subsequent casting, as the molten steel core still exists in the slab shell. However, because the slab shell is very thick, little broadening happens.

Using the square-root law of solidification, the fully solidified normal position and stagnant position can be derived, and thus the above three parts of the slab could be determined.

The slab was Q235 steel, the casting speed was 0.0167 $m \cdot s^{-1}$, the cross section of the slab was 2.050 m × 0.230 m, the upper width of the mold was 2.0813 m, the lower width of the mold was 2.0675 m, the casting temperature was 1533°C, T_l was 1513°C, and T_s was 1546°C.

The width of the front slab was also traced. It remained at 2.040 m, indicating that nearly no broadening of the slab happened at this position. It may be because it was cooled so rapidly that there was no time for broadening. Therefore, the width of the front slab was used as the standard width for assessing slab broadening.

The absolute broadening of the slab was derived from the slab width, which was measured while the slab was pushed through the exit of the continuous caster, subtracting the width of the front slab. The broadening values of the slab are shown in Figure 15(a) and (b).

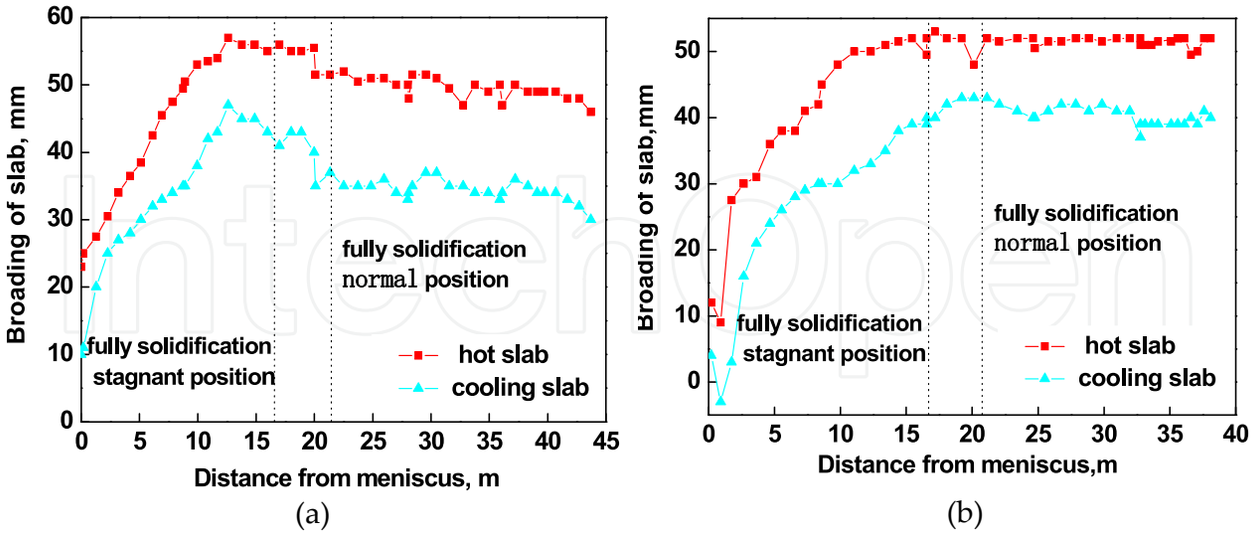

Figure 15. (a) Absolute broadening of slab in the first strand of stagnant slab; (b) Absolute broadening of slab in the second strand of stagnant slab.(FU JianXun et al.2011(a))

Slab broadening mainly happened in the front 6 segments (before 12.6 m). In these sectors, the broadening increases linearly with the distance from the meniscus. At the position of

12.6 m, the slab broadening was at its maximum, and then decreased slowly with distance from the meniscus. These results confirm that the stress of the roller is not the main reason for broadening. Otherwise, the slab broadening will happen before the slab is fully solidified near the 9th and 10th segments. The trend of slab broadening is consistent with that of the static pressure of molten steel, which confirms that the slab broadening is dependent on the static pressure of molten steel.

7. Mechanism of slab broadening

The static pressure of molten steel deforms the slab shell. The coupled thermo-mechanical viscoelastic-plastic 3D finite element model was built with the secondary development of the commercial software MSC.Marc. The calculated and measured results of slab width are shown in Figure 16.

The figure reveals that the calculated deformation agrees very well with the measured deformation. Slab broadening is the result of slab deformation under the pressure of static melting at high temperature. The deformation of the slab in the direction of thickness is shown in Figure 17(a). The temperature field of the slab is shown in Figure 17(b).

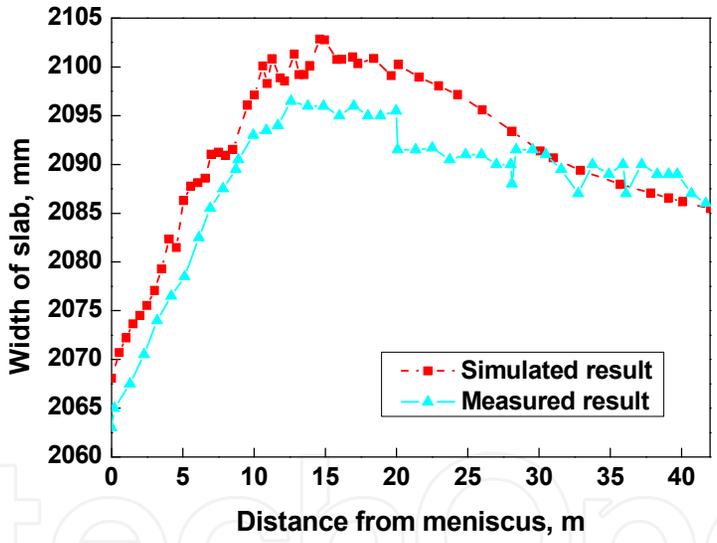

Figure 16. Simulated and measured widths of slab;(FU JianXun et al.2011(a))

The on-site investigation, force analysis, calculation from Maxwell creep model, and numerical simulation from the coupled thermo-mechanical viscoelastic-plastic 3D finite element model reveal that the slab broadening is due to slab deformation under the static pressure of molten steel. The slab shell deforms without constraints on the narrow side.

Creep deformation appears when the material plastic gradually deforms with time under certain conditions. Plastic deformation only happens when the stress exceeds the elastic limit. However, creep deformation happens when the acting time of stress is sufficiently long, even if the stress is very small. The creep deformation of metal is obvious only if the temperature is over the creep temperature (about 0.3 T_m). The slab deforms for a long time

under the pressure of static molten steel at high temperature. The creep rate depends on the composition of the compound metal, and the processes of refining and thermal treatment. Creep deformation causes slab broadening because it makes the material keep stress relaxed, reduces hardness, and enhances plasticity.

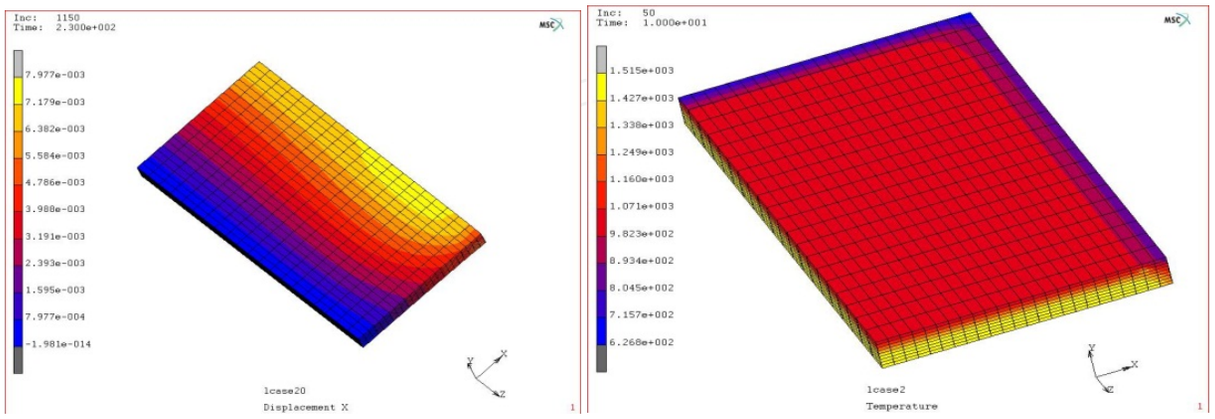

(a) (b)

Figure 17. (a) Deformation of slab in the direction of thickness at 230 mm; (b) Temperature field of slab at 1150 s. (FU JianXun et al. 2010(c))

The amount of broadening depends on the forces acting on the slab and the properties of the slab material, especially those at high temperature. Specifically, it depends on the static pressure of molten steel, the high-temperature mechanical properties of steel, the composition of the slab material, the thickness of the slab shell, secondary cooling intensity, casting speed, and the constitution of the caster.

The static pressure of molten steel is the driving force for the deformation of the slab shell. It is related to the type and constitution of caster. At present, vertical-bending casters are most common. For these casters, the static pressure is related to the density of molten steel and the height of the caster.

Under the conditions of high casting speed and constant cooling water, the fully solidified zone extend, the length of molten core increases, and the shell becomes thinner. Because of the higher temperature, the slab shell also has lower yield strength and better malleability. Consequently, the slab broadening increases. However, if the cooling water supply is changed when the casting speed is increased, the problem will become sophisticated.

The effects of steel grade on the broadening result from differences in material properties at high temperature, and hence differences in resistance to plastic deformation and creep deformation. With an increase in the carbon percentage, the ratio of ferrolite and austenite in the two phase regions changes. The increase in austenite is helpful to the reduction of slab broadening.

Intracell dislocation climb and intercell slide are two forms of creep deformation. Solution strengthening, precipitation strengthening, and dispersion strengthening insert a lot of defects into the crystal structure of steel, which hinder dislocation movement and thus

reinforce steel. Thus, micro-alloying of steel could enhance the hardness of the slab and reduce slab broadening.

In summary, higher casting speed, lower intensity of secondary cooling, thinner slab shell, larger static pressure of molten steel, and lower hardness of steel at high temperature increase slab broadening.

8. Conclusion

1. The mechanism of slab broadening is that the slab with high temperature exposes to no constraint at the direction of narrow face, and because of the static pressure of molten steel, the slab deforms in this direction.
2. Slab broadening is a common problem in continuous casting. The average RUB for the three grades of steel studied was in the range of 1.27%~3.00%, with a maximum of 4.4%.
3. Stagnant slab measurement experiments reveal that slab broadening happens in the 6 front segments, and that roller compaction is not responsible for slab broadening.
4. The agreement between the calculated results from the Maxwell model and the measured results illustrates that the Maxwell model is able to reveal the deformation behavior of a slab at high temperature.
5. Higher casting speed, lower intensity of secondary cooling, thinner slab shell, larger static pressure of molten steel, and lower hardness of steel at high temperature increase slab broadening. The micro-alloying of steel improves the hardness of the slab and reduces slab broadening.

Author details

Jian-Xun Fu and Weng-Sing Hwang
Research Center for Energy Technology and Strategy & Department of Materials Science and Engineering, National Cheng Kung University, Tainan 701, Taiwan

Acknowledgement

The authors gratefully acknowledge the guidance of Prof. Jingshe Li, Prof. Hui Zhang, Prof. Xingzhong Zhang, et al. The authors would like to thank the National Science Council of Taiwan (NSC100-2221-E-006-091-MY3) for funding this work.

9. References

Chen J. Hand Book of Continuous Casting (in Chinese). Beijing: Metallurgical Industry Press, 1990,

Fu JianXun, Li Jingshe, Zhang Hui, Zhang Xing-zhong. Industrial Research on broadening of slab in continuous casting. JOURNAL OF RON AND STEEL RESEARC INTERNATIONAL. 2010. 17(8):20-24,

Fu JianXun, Li Jingshe, Zhang Hui, Zhang Xingzhng, Mechanism of broadening of slab in the secondary cooling zone of continuous casting. SCIENCE CHINA- Technological Sciences. 54 (2011), No.5: 1228–1233,

Fu JianXun, LI Jingshe, ZHANG Hui,. Effects of Width and Thickness of Sab on Broadening in Continuous Casting. International Journal of Minerals, Metallurgy and Materials. 17 (2010), No. 6, 723,

Fu JianXun, Li Jingshe, Zhang Hui, Viscoelastic–Plastic Analysis of Broadening of Slab in the Secondary Cooling Zone of Continuous Casting. Acta Metallurgica Sinica, 46 (2010), No. 1, 91-96 (in chinese),

Jian-Xun Fu, Weng-Sing Hwang, Jing-she Li, and Zhang Hui. Effect of Casting Speed on Slab Broadening in Continuous Casting. steel research int. 2011 (82) No. 11. 1266- 1272,

I.Ohnaka. Mathematical Analysis of solute redistribution during solidification with diffusion in solid phase. Transactions of ISIJ, 1986, 26: 1045-1051,

K. Sorimachi, J. K. Brimacombe: Ironmak Steelmak, 1977; 4: 240,

Lei H, Yang L D, Zeng J, et al. Discussion of computational methods for the forces incurred in the bending phase in slab casting (in Chinese).Heavy Mach, 2007, (3): 41–45,

Lin Q Y, Jiang H J, Zhu M Y. Analysis of reduction parameters of dynamic soft reduction in continuous casting. J Mater Metall, 2004, 3(4): 261–265,

Miyazawa K, Schwerdtfeger K. Computation of Bulging of Continuously Cast Slab With Simple Bending Theory. Ironmaking and Steelmaking, 1979(2) : 68,

Mizukami H , Murakami K, Miyashita Y. Mechanical Proper ties of Continuously Cast Steel at High Temperatures [J]. Tetsu-to-Hagane. 1977. 63: 146 (in Japanese),

Ramacciotti A. Thermo-Mechanical Behavior of the Solidified Shell in a Funnel-Shaped Mold for Continuous Casting of Thin Slabs rJ1. Steel Research, 1988. 5gr 438,

Sheng Y, Sun J, Zhang M. Calculation for bulging deformation of continuously casting slab (in Chinese). Iron Steel, 1993, 28(3): 20–25,

S. Kobayashi, T. Nagamichi and K. Gunji: Transactions of ISIJ, 28(1988), 543,

Sun J, Sheng Y, Zhang X. Analysis of bulging deformation and stress in continuous cast slabs (in chinese). J Iron Steel Res, 1996, 8 (1): 11–15,

Uehara M. Samarasekera I V, Brimacornbe J K. Mathematical Modeling of Unbending of Continuously Cast Steel Slabs. Ironmaking and Steelmaking, 1986(12) : 138,

Ueshima Y, Mizoguchi S, Matsumiya T, et al. Analysis of solute distribution in dendrites of carbon steel with δ/γ transformation during solidification. Metallurgical and Materials Transactions B, 1986, 17B(4): 845-859,

Xiong Yi-gang. Continuous Casting of Slab [M]. Beijing: Metallurgical Industry Press, 1994 (in Chinese),

Y. S. Xi and H. H. Chen: MSC.Marc Manual for Analysis Using Temperature Field and the Coupled Field, MSC. Software user manual, 2001 (Iin Chinese),